International Journal of Thermal Sciences 102 (2016) 47–61

Contents lists available at ScienceDirect

International Journal of Thermal Sciences

journal homepage: www.elsevier.com/locate/ijts

Quasi-online parametric identification of moving heating devices in a 2D geometry

Alban Vergnaud [a], Laetitia Perez [b], Laurent Autrique [a, *]

[a] LARIS – ISTIA, University of Angers, 62 Avenue Notre Dame du Lac, 49000 Angers, France
[b] LTN-IUT, University of Nantes, La Chantrerie, Rue Christian Pauc, BP50609, 44306 Nantes, Cedex 03, France

ARTICLE INFO

Article history:
Received 29 October 2014
Received in revised form
23 May 2015
Accepted 14 October 2015
Available online xxx

Keywords:
Parametric identification
Regularization method
Conjugate gradient method
Online parameters estimation
Sliding time window
Partial differential equations

ABSTRACT

This work is devoted to an adaptation of the conjugate gradient method for the identification of heat flux densities provided by two mobile sources on a two-dimensional geometry. This adaptation is based on a sliding-time window in order to achieve quasi-online identification of unknown time-dependent parameters. The proposed method ensures sequential in time iterative regularization in order to deal with the ill-posed nature of inverse heat conduction problem (IHCP). The studied configuration is issued from experimental reflections in order to investigate a practical case. A set of fixed sensors is considered while heating sources trajectories are accurately known. Measurements provided by sensors are disturbed according to a realistic Gaussian noise. Several strategies are detailed in this communication (adaptive integration interval, sliding time window, initialization improvement, choice of the sliding window size). In each situation, the benefit in terms of delay reduction is discussed in regards with the identification accuracy. It is shown that such methodology provides an attractive procedure consistent with adaptive control aims and real time signal processing.

1. Introduction

In engineering sciences, real processes are frequently modelled in order to predict and to act on these systems. However, some parameters are often unknown considering the phenomena complexity. Thus, an identification procedure has to be implemented to estimate these parameters in order to develop an accurate model. In thermal sciences, characteristics of inverse problems and their numerical resolution are investigated in Refs. [3,4,29,32]. For situations where forward problems and inverse problem are described by partial differential equations (PDE), several studies can be cited [2] and [17]. In numerous references, parameter estimation for heat flux identification is achieved considering numerical resolution of inverse problems [33,15,21,14]. In this context it is usual to wait the recording of all measurements before starting the identification procedure (usually based on a minimization algorithm for the quadratic cost function related to the difference between simulated temperatures and measurements). However, such offline approach is not adapted for process control or diagnosis purposes (to maintain or increase the process dependability). Thus, if the inversion is implemented with the intention of performing online identification, reduction of the calculation time is essential.

In such a framework, in Ref. [26] sequential approaches are analysed considering the well-known Beck's method. Piecewise-constant approximation of the unknown parameter is considered in a 1D geometry with a single sensor used for time dependant heat flux identification (Neumann condition). The time interval is subdivided in equal time steps and several numbers of “future times” are taken into account. Minimization algorithm is based on Newton's method. In Ref. [27], in a 1D geometry, a sequential variant of the conjugate gradient methods proceeds similarly to the Beck's method. Unknown parameters are the initial temperature and the heating flux on a boundary.

Sequential approach is also implemented in Ref. [11] for a 2D geometry with an unknown heat flux on a part of the domain boundary. Tikhonov regularization is performed in order to deal with the ill-conditioned nature of the inverse problem. The gradient method is considered for cost function minimization. Temperatures are measured using 11 sensors and measurements errors are taken into account. In Ref. [31], a sequential procedure based on future time steps is implemented in order to perform model reduction. Such technique is based on a proper selection of

* Corresponding author.
E-mail addresses: alban.vergnaud@univ-angers.fr (A. Vergnaud), laetitia.perez@univ-angers.fr (L. Perez), laurent.autrique@univ-angers.fr (L. Autrique).

http://dx.doi.org/10.1016/j.ijthermalsci.2015.10.019
1290-0729/

Nomenclature

General symbols

C	specific heat capacity, J kg^{-1} K^{-1}
e	thickness, m
h	heat transfer coefficient, W m^{-2} K^{-1}
I	disk center
l	plate width, m
L	plate length, m
max_{err}	maximum error on heat flux density estimation, W m^{-2}
$\overrightarrow{n}$	unit external outward-pointing vector
N_C	total number of sensors
N_t	number of time interval for identification
$N_{\mathscr{F}}$	number of identification problems resolution
$r_{j=1,2}$	heat flux radius, m
$s^i(t)$	basis function for piecewise linear functions
$\overline{s(t)}$	vector of basis function $s^i(t)$
t	time, s
t_{id}	identification time, s
t_f	final time, s
x	space variable, m
y	space variable, m

Greek symbols

λ	thermal conductivity, W m^{-1} K^{-1}
μ_{delay}	average delay on the identification, s
μ_{res}	average temperature residual, K
μ_{err}	average heat flux density estimation errors, W m^{-2}
$\phi(t)$	heat flux density, W m^{-2}
$\overline{\phi_j}$	vector related to source j heat fluxes in W m^{-2}
ρ	density, kg m^{-3}
σ_{res}	standard deviation of temperature residual, K
σ_{err}	standard deviation of heat flux density estimation errors, W m^{-2}
θ	temperature, K
θ_0	initial temperature, K

Subscript

0	initial
i	for sensors
j	for heating sources

Superscript

i	related to time discretization
k	iteration
tr	matrix transpose

eigenmodes (dominant) of the state matrix in order to reduce the system dimension. Studied geometries are 2D or 3D and it is shown that once the different elementary reduced models were built, identification is rather fast.

Implementation of an extended Kalman filter for identification purposes related to IHCP is proposed for example in Refs. [9,10]. Such technique, well known in signal processing, induces time-lag on identified parameters and can be difficult to tune without a priori information (related to the noise distribution for example). Configurations studied in both previous references are related to boundary heat flux identification considering a 1D mathematical model.

In Ref. [12], recent investigations in a 3D domain are performed in order to identify a surfacic heat flux using 36 micro-thermocouples located quite closely underneath the investigated surface. A conjugate gradient method is performed for criterion iterative minimization and a weak formulation based on Galerkin finite-dimensional technique. A multilevel approach is mentioned in order to consider sequential identification for the acceleration of minimizing the Tikhonov functional (but there are no details related to numerical implementation or tests).

Recently, a “building block” approach has been proposed in Ref. [23] in order to identify a boundary heat flux (depends on the space variable but constant versus time) in a two dimensional geometry. The proposed technique is based on 2D transient Green's function solution equation. Unknown heat flux spatial profile is assumed to be piecewise constant. Such attractive method seems to be difficult to implement in general cases with complex geometries, non linearities and disturbed measurements.

In the following, the numerical resolution of an inverse heat conduction problem in a 2D geometry is investigated in order to perform a quasi-online identification of mobile surfacic heat fluxes. Considering the previous methods and in order to prevent the bias occurred by extended Kalman filter (time-lag) or by the function specification such as Beck's sequential method (for which the use of future times information induces bias in the estimate for the unknown heat flux) a different method is proposed. The proposed approach is based on an adaptation of a regularization method: the conjugate gradient method (CGM). Such method is widespread in offline context and well known for inverse heat conduction problem [18,19,28,5]. In the studied context, the aim is to reduce computational time in order to obtain identification results on time interval $[t_0,t_1]$ as fast as possible after the measurement availability ($\approx t_1$). Then the overall method is developed in the aim of delay reduction under the constraint of a reliable identification. Such objective is also related to optimal trajectories strategies for mobile sensor [7,24] which can be implemented using the experimental prototype described in [30] (based on mobile robots and vision system [20,34]). Adaptative control for time-delay systems [13] is also concerned by ths approach. Identification is sequentially performed on sliding time windows in order to adapt the integration interval and to provide overlap which can avoid identification bias. The regularization is ensured considering the admissible level of minimization [2]: iteration number acts as a regularization parameter.

In the following paragraph the forward problem is described. The partial differential equation system is exposed and the mobile sources trajectories are given. Several numerical results are shown considering a finite element method. Then in the third paragraph, inverse problem is exposed and the main steps of CGM are briefly given considering the sensitivity problem and the adjoint problem. Then numerical results are shown in order to investigate the effect of the adapted method in comparison with the offline approach. Several strategies are implemented and compared (adaptive, sliding time window, initialization improvement, choice of the sliding window size). The robustness will be put on view for each proposed strategies. Effects on both delay reduction and identification accuracy are shown.

2. Direct problem

Let us consider two mobile heating sources, S_1 and S_2, moving on a thin metallic rectangular plate $\Omega = \left[\frac{-L}{2},\frac{+L}{2}\right] \times \left[\frac{-l}{2},\frac{+l}{2}\right] \subset \mathbb{R}^2$, with boundaries $\partial\Omega \in \mathbb{R}$ and thickness e. For each source, the heat flux

density $\phi_j (j = 1,2)$ is considered as spatially uniform on a mobile disk $D_j(I_j,r_j)$ with center $I_j(x_j,y_j)$ and radius r_j. The total heat flux applied on the plate at every moment can be written:

$$\Phi(x,y;t) = \begin{cases} \phi_1(t) & if \ \ (x,y) \in D_1(I_1(t), r_1) \\ \phi_2(t) & if \ \ (x,y) \in D_2(I_2(t), r_2) \\ 0 & \text{otherwise} \end{cases} \quad (1)$$

To describe these two heat fluxes in continuous and differentiable way, spatial regularization is used and the total heat flux can be expressed as follow:

$$\Phi(x,y;t) = \sum_{j=1}^{2} \frac{\phi_j(t)}{\pi} \left(-\arctan(A_j(x,y)) + \frac{\pi}{2} \right) \quad \text{with}$$
$$A_j(x,y) = \mu \left(\sqrt{(x-x_j)^2 + \left(y-y_j\right)^2} - r_j \right) \quad (2)$$

The parameter $\mu \in \mathbb{R}^+$ has been chosen to deal with heat flux discontinuity. The time interval $T = [0,t_f]$ can be divided into N_t segments $T = \cup_{i=0}^{N_t-1} [t_i, t_{i+1}]$ with $t_i = \tau i$ and a discretization step defined by $\tau = t_f/N_t$. Without loss of generalities, the unknown heat flux densities $\phi_1(t)$ and $\phi_2(t)$ can be formulated as piecewise continuous linear functions and can be written considering basis functions $s^i(t)$ for $i = 0,\ldots,N_t$:

$$s^i(t) = \begin{cases} \frac{t}{\tau} - i + 1 & \text{if} \quad t \in [t_{i-1}, t_i] \\ -\frac{t}{\tau} + i + 1 & \text{if} \quad t \in [t_i, t_{i+1}] \\ 0 & \text{otherwise} \end{cases}$$

The two heat flux densities are then expressed as follows: $\phi_j(t) = \sum_{i=0}^{N_t} \phi_j^i s^i(t) = (\overline{\phi_j})^{tr} \overline{s(t)}$.

Considering that the plate is thin, temperature gradient versus the plate thickness (e) can be neglected and a two dimensional mathematical model is validated. Both heat losses (convective exchanges are similar on the lower and the upper face) and heating fluxes are formulated in the heat equation (issued from energy balance considering Fourier's law). Thus, temperature $\theta(x,y;t)$ within the domain is solution of PDE system (3). Thermal conductivity λ in this study is considered not dependent of the temperature, of the spatial distribution and of time.

The source term $\Phi(x,y;t) - 2h(\theta(x,y;t) - \theta_0)/e$, expressed in (W m^{-3}), is relevant if thickness e is small enough. In the studied configuration, according to the heat fluxes range and to the parameters taken into account in the studied case, a previous numerical study has shown that the 2D model is valid in comparison with the 3D domain (a parallelepiped with a surfacic heat flux $\phi(.)$ on a face).

3. Inverse problem

3.1. Formulation

To estimate the heat flux densities $\phi_1(t)$ and $\phi_2(t)$ from temperature evolutions provided by sensors located on the plate, an inverse problem can be formulated and solved by minimizing the following quadratic criterion (4). This criterion describes the quadratic difference between simulated temperature $\theta(C_i,t;\overline{\Phi})$ (direct problem solution (3) for sensor C_i with the estimation of the heat flux densities $\overline{\Phi} = (\overline{\phi}_1 \quad \overline{\phi}_2) \in \mathbb{R}^{2N_t}$) and the measured temperature $\widehat{\theta}_i(t)$ provided by sensor C_i (noisy simulated measurements).

$$J(\theta, \overline{\Phi}) = \frac{1}{2} \sum_{i=0}^{N_c} \int_0^{t_f} \left(\theta(C_i,t;\overline{\Phi}) - \widehat{\theta}_i(t) \right)^2 dt \quad (4)$$

The conjugate gradient method is implemented to identify the unknown parameters [18,25,32]. This algorithm requires iterative resolution of three well-posed problems: the direct problem (3) to calculate the cost-function $J(\theta, \overline{\Phi}^k)$ and estimate the quality of the estimate $\overline{\Phi}^k$ at iteration k; the sensitivity problem to calculate the descent depth (in the descent direction); the adjoint problem to determine the gradient of the cost-function $J(\theta, \overline{\Phi})$ and thus to define the next descent direction [6,16].

3.2. Sensitivity problem

Let us consider $\delta\theta(x,y;t)$ the temperature variation induced by heat flux densities variations. $\delta\theta(x,y;t)$ is solution of the following system:

$$\begin{cases} \forall (x,y;t) \in \Omega \times T & \rho c \dfrac{\partial \theta(x,y;t)}{\partial t} - \lambda \Delta \theta(x,y;t) = \dfrac{\Phi(x,y;t) - 2h(\theta(x,y;t) - \theta_0)}{e} \\ \forall (x,y) \in \Omega & \theta(x,y;0) = \theta_0 \\ \forall (x,y;t) \in \partial\Omega \times T & -\lambda \dfrac{\partial \theta(x,y;t)}{\partial \vec{n}} = 0 \end{cases} \quad (3)$$

$$\begin{cases} \rho c \dfrac{\partial \delta\theta(x,y;t)}{\partial t} - \lambda \Delta \delta\theta(x,y;t) = \dfrac{\delta\Phi(x,y;t) - 2h\delta\theta(x,y;t)}{e} & \forall (x,y;t) \in \Omega \times \left[0, t_f\right] \\ \delta\theta(x,y;0) = 0 & \forall (x,y) \in \Omega \\ -\lambda \dfrac{\partial \delta\theta(x,y;t)}{\partial \vec{n}} = 0 & \forall (x,y;t) \in \partial\Omega \times \left[0, t_f\right] \end{cases} \quad (5)$$

with

$$\delta\Phi(x,y;t)=\sum_{j=1}^{2}\frac{\delta\phi_j(t)}{\pi}\Big(-\arctan\big(A_j(x,y)\big)+\frac{\pi}{2}\Big)$$

$$=\frac{1}{\pi}\sum_{j=1}^{2}\Big(\overline{\delta\phi_j}\Big)^{tr}\overline{s(t)}\Big(-\arctan\big(A_j(x,y)\big)+\frac{\pi}{2}\Big) \tag{6}$$

The solution $\delta\theta(x,y;t)$ of the sensitivity problem is used to calculate the descent depth at each iteration k:

$$\gamma^k=\underset{\gamma\in\mathbb{R}}{\mathrm{Arg\,min}}\,J\Big(\overline{\Phi}-\gamma d^k\Big)$$

$$=\frac{\displaystyle\int_0^{t_f}\sum_{i=1}^{N_c}\Big(\theta\Big(C_i,t;\overline{\Phi}^k\Big)-\widehat{\theta}_i(t)\Big)\delta\theta\Big(C_i,t;\overline{\Phi}^k\Big)dt}{\displaystyle\int_0^{t_f}\sum_{i=1}^{N_c}\Big[\delta\theta\Big(C_i,t;\overline{\Phi}^k\Big)\Big]^2dt} \tag{7}$$

The descent direction $d^k\in\mathbb{R}^{2N_t}$ is defined according to the conjugate gradient algorithm and depends on the cost-function gradient.

3.3. Adjoint problem

In order to determine the gradient of the cost-function $\nabla J^k=\begin{pmatrix}\frac{\partial J}{\partial\phi_1^{i,k}}\\ \frac{\partial J}{\partial\phi_2^{i,k}}\end{pmatrix}_{i=(1,\dots,N_t)}$ at each iteration k of the minimization algorithm, a Lagrangian formulation $\ell(\theta(x,y;t),\Phi,\psi)$ is introduced:

$$\ell(\theta,\Phi,\psi)=J(\theta,\Phi)+\int_0^{t_f}\int_\Omega\Big(\rho c\frac{\partial\theta(x,y;t)}{\partial t}-\lambda\Delta\theta(x,y;t)-\frac{\Phi(x,y;t)}{e}+\frac{2h(\theta(x,y;t)-\theta_0)}{e}\Big)\psi dtd\Omega \tag{8}$$

The Lagrangian variation is written as follows:

$$\delta\ell(\theta,\Phi,\psi)=\frac{\partial\ell(\theta(x,y;t),\Phi,\psi)}{\partial\theta(x,y;t)}\delta\theta+\frac{\partial\ell(\theta(x,y;t),\Phi,\psi)}{\partial\Phi}\delta\Phi+\frac{\partial\ell(\theta(x,y;t),\Phi,\psi)}{\partial\psi}\delta\psi$$

Lagrangian variation could also be written:

$$\delta\ell(\theta,\Phi,\psi)=\int_0^{t_f}\sum_{i=1}^{N_c}\Big(\theta(x_i,y_i;t;\overline{\Phi})-\widehat{\theta}_i(x_i,y_i;t)\Big)\delta\theta(x_i,y_i;t)dt$$

$$+\int_0^{t_f}\int_\Omega\Big[\rho c\frac{\partial\delta\theta(\cdot)}{\partial t}-\lambda\Delta\delta\theta(\cdot)-\frac{\delta\Phi-2h\delta\theta(x,y;t)}{e}\Big]\psi(\cdot)dtd\Omega$$

Let us consider that $\psi(x,y;t)$ is fixed such that: $\delta\ell(\theta,\Phi,\psi)=\frac{\partial\ell(\theta(x,y;t),\Phi,\psi)}{\partial\Phi}\delta\Phi$

Then, considering equations of previous sensitivity problem (5), $\psi(x,y;t)$ is solution of problem (9):

$$\begin{cases}\forall(x,y;t)\in\Omega\times\big[0,t_f\big] & \rho c\dfrac{\partial\psi(x,y;t)}{\partial t}+\lambda\Delta\psi(x,y;t)=E(x,y;t)+\dfrac{2h\psi(x,y;t)}{e}\\ \forall(x,y)\in\Omega & \psi\Big(x,y;t_f\Big)=0\\ \forall(x,y;t)\in\partial\Omega\times\big[0,t_f\big] & -\lambda\dfrac{\partial\psi(x,y;t)}{\partial\overrightarrow{n}}=0\end{cases} \tag{9}$$

with $E(x,y;t)=\sum_{i=1}^{N_c}(\theta(x_i,y_i;t;\overline{\Phi})-\widehat{\theta}_i(x_i,y_i;t))\ \delta_{D,C_i}$ and $\delta_{D,Ci}$ is the Dirac distribution for sensor $C_i(x_i,y_i)$. When $\psi(x,y;t)$ is solution of the adjoint problem (9) then, $\delta\ell(\theta,\Phi,\psi)=\frac{\partial\ell(\theta(x,y;t),\Phi,\psi)}{\partial\Phi}\delta\Phi=\delta J(\theta,\Phi)$

$$\delta J(\theta,\Phi)=-\int_0^{t_f}\int_\Omega\Big[\frac{\delta\Phi(x,y;t)\psi(x,y;t)}{e}\Big]d\Omega.dt=-\int_0^{t_f}\int_\Omega\frac{1}{e}\Big[\sum_{j=1}^{2}\frac{\delta\phi_j(t)}{\pi}\Big(-\arctan\big(A_j(x,y)\big)+\frac{\pi}{2}\Big)\Big]\psi(x,y;t)d\Omega.dt \tag{10}$$

Thus, the gradient is expressed by:

$$\text{For } j=1,\ 2 \quad \frac{\partial J}{\partial \phi_j^i} = -\int_0^{t_f}\int_\Omega \frac{s^i(t)}{\pi}\left(-\arctan(A_j(x,y))+\frac{\pi}{2}\right)\left[\frac{\psi(x,y;t)}{e}\right]d\Omega.dt \tag{11}$$

4. Numerical results

4.1. The studied case

The investigated domain is shown in (Fig. 1). Trajectories of both disks centres ($I_1(t)$,$I_2(t)$) are given in this figure (initial locations is determined at $t=0$). Model parameters are shown in Table 1.

In order to obtain simulated measurements, two realistic heat fluxes $\phi_1(t)$ and $\phi_2(t)$ are considered (Fig. 5). Numerical resolutions presented in this communication are based on the finite elements method implemented with Comsol® software interfaced with Matlab©. In this study, the elements used are triangles and the interpolation functions are quadratic. The number of degrees of freedom is 4749. Previous studies have shown that in the studied case, such numerical scheme is in adequacy with the desired accuracy. It is obvious that a coarser mesh would reduce the computational time (which is the key goal for online identification) but is meaningless if numerical solutions are erroneous. Numerical resolutions are performed on a personal computer whose characteristics are: CPU: Intel® Core™ i7-3520M CPU @ 2.90 GHz, RAM: 8.00 Go, OS: Windows 7 (64).

Temperature evolution for each sensor $C_{i=1,\cdots,10}$ is calculated with the known parameters listed in Table 1 and results for these simulated measurements are shown in (Fig. 2). Different temperature spatial distributions at time 150 s, 300 s, 450 s and 600 s are presented (Fig. 3).

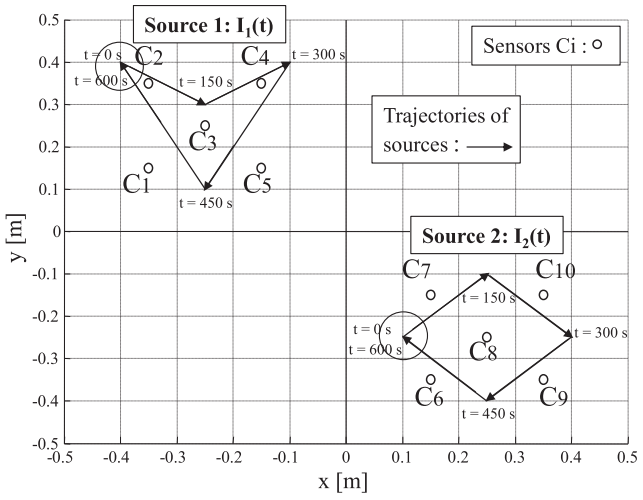

Fig. 1. Direct problem representation.

Table 1
Model parameters.

ρc (J m^{-3} K^{-1})	2,43.10^6	e (m)	$2\cdot10^{-3}$
$r_{j=1,2}(m)$	$6\cdot10^{-2}$	h (W m^{-2} K^{-1})	10
L=$l(m)$	1	t_f (s)	600
λ (W m^{-1} K^{-1})	160	θ_0 (K)	291

4.2. Conjugate gradient method and offline identification

For algorithm initialization $k=0$, let us consider the following heat flux densities $\phi_1^k(t)=\phi_2^k(t)=0 \quad (\forall t\in T)$. Conjugate gradient method is implemented in order to identify the heat flux density of these two mobile sources considering noisy measurements (N(0,0.5)) obtained for 10 sensors. Sensors locations are shown in Fig. 1 while temperature evolution without noises are presented in Fig. 2. The cost-function versus iteration number is presented in (Fig. 4). The identification has converged in 82 min with a stop-criterion $J_{Stop}=0.5N_sN_t\sigma^2$ [1].

The two identified heat fluxes are represented in (Fig. 5).

To validate these two identified heat densities, temperature residual between real data and simulated data are presented in Table 2.

In order to evaluate the identification quality, the average μ_{err}, the standard deviation σ_{err} and the maximum max_{err} of errors between estimated and real heat flux density are presented in Table 3.

Results presented Tables 2 and 3 show that such offline identification technique is efficient: residual temperatures are acceptable and considering the heat fluxes ranges (Fig. 5) average error on identified are quite small. Offline CGM successfully deals with disturbed measurements and with a great number of unknown parameters: 118 parameters are required to identify heat fluxes every 10 s considering that both initial and final fluxes are known. Since results are obtained 82 min after the measurements end ($t_f=10$ minutes) an adapted online method is proposed in the following.

4.3. Quasi-online identification

Previous results highlight the efficiency of the conjugate gradient method. However heat flux densities are identified after 82 min while numerical experiment duration is 10 min. The main inconvenient of this method is the convergence time which can be very important according to the problem complexity. Thus, the strategy for the choice of the time interval related to identification purpose is crucial. In the following several methods are proposed and compared. Let us consider notations about time definition. Experimental time is denoted by $t_{\exp}$ and can be considered as real-time which start at $t=0$ s. At each second a new measurement is obtained. After 600 s, experimentation is stopped. Identification time is denoted by t_{id} and can be considered as the instant for which an identification result is obtained. This can be roughly illustrated with 3 strategies for experimentation duration equal to 10 min (=600 s):

- S–A: identification algorithm is launched and identification results are obtained after 82 min. This is offline approach presented in previous paragraph.
- S–B: identification algorithm is launched every 60 s and identification duration is less than 60 s. In such a case, identification algorithm has always to wait for new measurements.
- S–C: identification algorithm is launched every 10 s and identification duration is greater than 10 s. In this situation, identification algorithm is always late and is launched as soon as the previous identification is finished (measurements are available).

These strategies are shown in Fig. 6. Total delay is the difference $\Delta_{tot}=t_{id}-t_{\exp}$ when all the measurements have been taken into account for identification. Running delay $\Delta_{run}=t_{id}-t_{\exp}$ is the delay

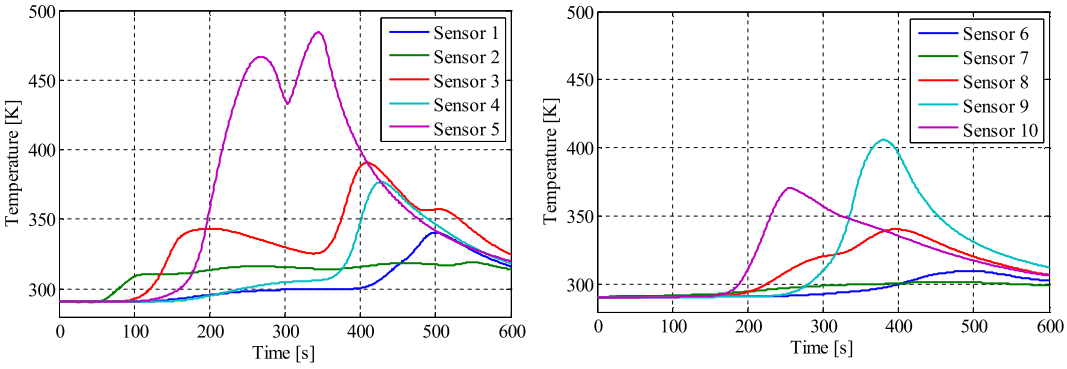

Fig. 2. Temperature evolution for sensors $C_{i=1,\cdots,5}$ (left) and sensors $C_{i=6,\cdots,10}$ (right).

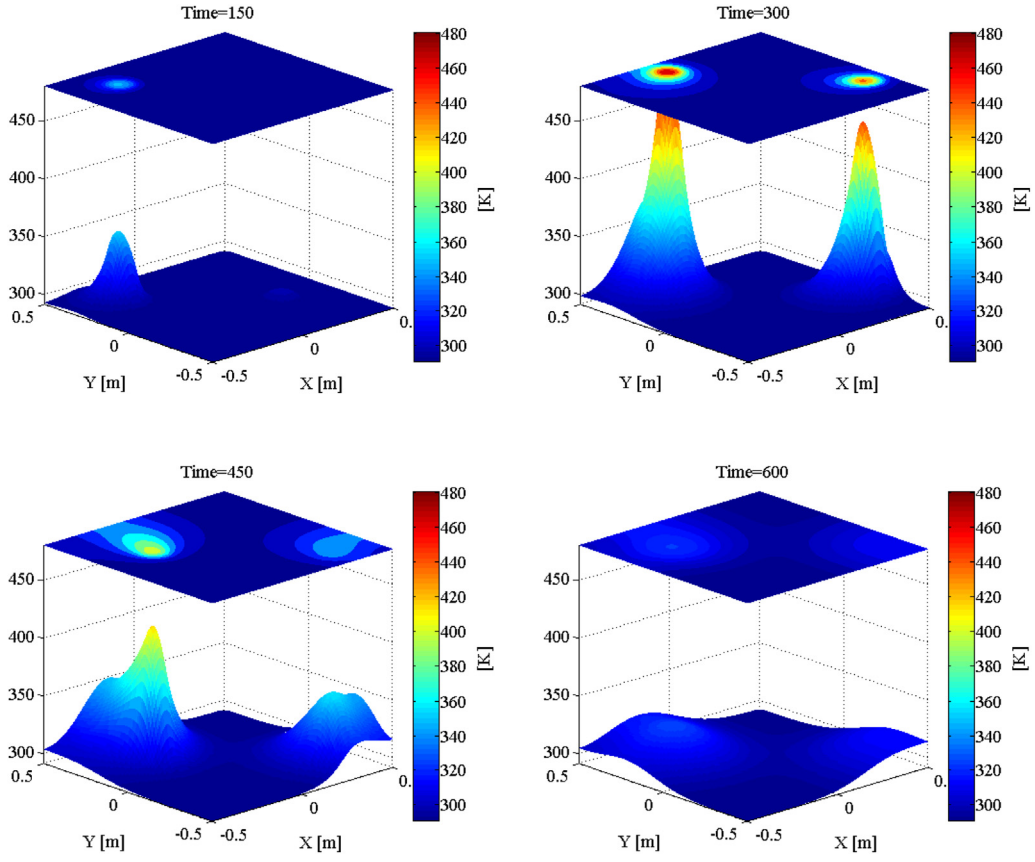

Fig. 3. Temperature spatial distribution for several times.

corresponding to an identification achievement based on last measurements. Examples are presented in Fig. 6:

- Strategy S–A: $\Delta_{tot} = \Delta_{run} = 82$ minutes
- Strategy S–B: $\Delta_{tot} < 60$ seconds and $\Delta_{run} < 60$ seconds
- Strategy S–C: $\Delta_{tot} = 522$ seconds and $\Delta_{run} < 20$ seconds

It is obvious that offline strategy S-A presented in previous paragraph 4.2 induces a very important delay. The faster strategy should be S–B but it is not possible to develop such approach and in practice, according to the unknown parameters variations (and to their sensitivity on measurements) identification algorithm behaviour can change between S–B and S–C during the same experimentation. In the following, several approaches are detailed.

Adaptation of the principle of the conjugate gradient method algorithm is implemented considering time intervals for identification $\mathscr{T}_i = [\tau_i^-, \tau_i^+] \subset T$ which will slide on the total time horizon with a step $0 < \Delta t_i < \tau_i^+ - \tau_i^-$ to identify the values of unknown parameters $\phi_1^{\mathscr{T}_i}(t)$, $\phi_2^{\mathscr{T}_i}(t)$ on each interval $\mathscr{T}_i$.

The offset $\Delta t_i \leq \tau_i = \tau_i^+ - \tau_i^-$ is chosen in order to ensure that there is an overlap between two successive time windows $\mathscr{T}_i = [\tau_i^-, \tau_i^+]$ and $\mathscr{T}_{i+1} = [\tau_{i+1}^-, \tau_{i+1}^+]$. This overlap is a crucial

requirement in order to avoid bias occurred by measurements noises and to overcome the usual fact that it is quite difficult to identify an unknown heat flux on $\mathscr{T}_i = [\tau_i^-, \tau_i^+]$ considering that the last measurement is obtained at τ_i^+. In practice, the last value is not accurately identified. The overlap overcomes this difficulty.

When the values of the parameters are accurately estimated on $\mathscr{T}_i$ (or the iteration number is greater than a maximum number), the identification window is translated on a new time interval $\mathscr{T}_{i+1} = [\tau_i^- + \Delta t_i^-, \tau_i^+ + \Delta t_i^+] = [\tau_{i+1}^-, \tau_{i+1}^+]$ considering initialization:

$$\forall t \in \mathscr{T}_{i+1} = \left[\tau_{i+1}^-, \tau_{i+1}^+\right]:$$
$$\phi_{1,\mathscr{T}_{i+1}}^{k=0}(t) = \begin{cases} \phi_{1,\mathscr{T}_i}(t) & \text{if} \quad t \le \tau_i^+ \\ \phi_{1,\mathscr{T}_i}\left(\tau_i^+\right) & \text{if} \quad t > \tau_i^+ \end{cases} \quad \text{and} \quad (12)$$
$$\phi_{2,\mathscr{T}_{i+1}}^{k=0}(t) = \begin{cases} \phi_{2,\mathscr{T}_i}(t) & \text{if} \quad t \le \tau_i^+ \\ \phi_{2,\mathscr{T}_i}\left(\tau_i^+\right) & \text{if} \quad t > \tau_i^+ \end{cases}$$

The different steps of resolution algorithm to implement quasi-online identification are presented below.

In the next paragraphs, several strategies based on this approach are proposed and analysed.

4.3.1. Strategy 1: constant offset with constant time window size

For this first strategy, the time interval of the window $\mathscr{T}_i = [\tau_i^-, \tau_i^+] \subset T$ used to identify $\phi_{1\ \mathscr{T}_i}(t)$, $\phi_{2\ \mathscr{T}_i}(t)$ is fixed at a constant interval $\tau_i^+ - \tau_i^- = 60\ s$ (10% of the overall time of experimentation). This first strategy is based on a constant offset of $\mathscr{T}_i$ with $\Delta t < \tau_i^+ - \tau_i^-$ to ensure identification ranges overlap. Initially an offset value $\Delta t = 15$ s (25% of time interval $\mathscr{T}_i$) is studied, the results of the identification of the two heating flux densities are presented in Table 5. The convergence of this identification is obtained after about $t_{id} = 24$ min (i.e. $\Delta_{tot} = 14$ min after the end of the measurements recording). To compare with the offline CGM, several offsets have been tested (Table 5). The number of time interval $\mathscr{T}_i$ is $N_T = \frac{540}{\Delta t} + 1$. The delay Δ_{run} between a measurement at time t_{exp} and the determination of the heat fluxes ($\phi_1(t_{exp})$,$\phi_2(t_{exp})$) obtained at time t_{id}, is presented Fig. 7. Since measurements are obtained each seconds, 600 delays are estimated. Average delay on the identification is denoted by μ_{delay}.

1) Solve direct problem on interval $\mathscr{T}_i$

2) Compute cost function with estimated temperature values on interval $\mathscr{T}_i$ and associated measurements.

If the criterion is lower than the stop criterion or the maximum number of iteration is reached, then identification on the interval $\mathscr{T}_i$ is stopped and a new time interval $\mathscr{T}_{i+1}$ is considered (goto step 1 with $i = i+1$.)

else

3) Solve the adjoint problem on interval $\mathscr{T}_i$

4) Compute the descent directions on the time interval $\mathscr{T}_i$ considering the cost function gradient issued from previous adjoint problem resolution.

5) Solve sensitivity problem on interval $\mathscr{T}_i$ to calculate the descent depth (in the descent direction)

6) Update new estimations of unknown parameters which are estimated on the time interval $\mathscr{T}_i$; Goto step 1.

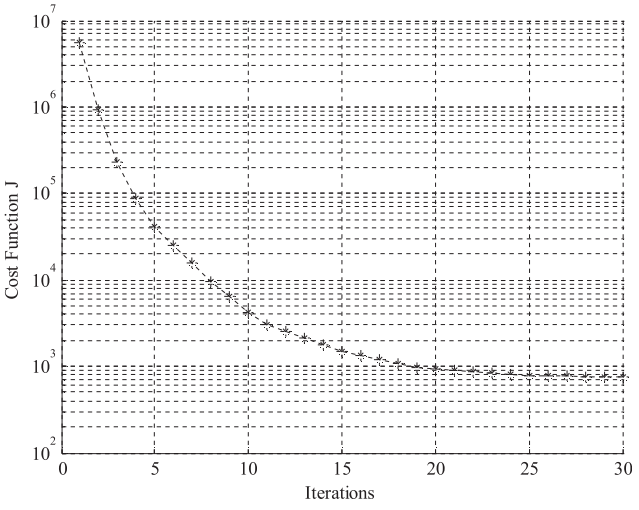

Fig. 4. Criterion evolution.

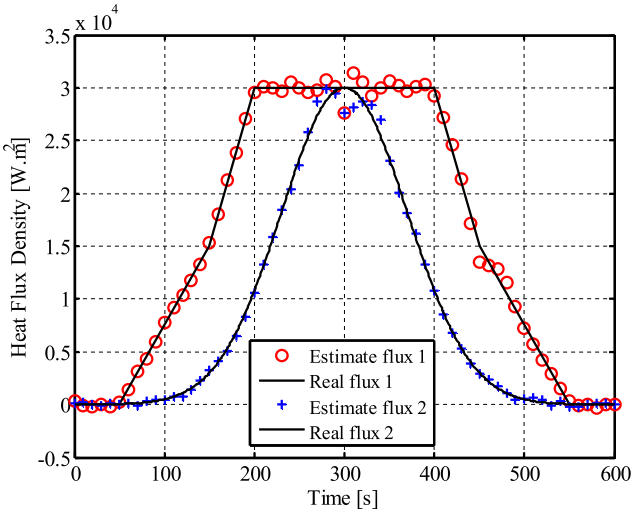

Fig. 5. Estimate heat flux densities (Sources 1 & 2).

If Δt increases (overlap decreases), the number of inverse problem is reduced and the average delay is reduced. In order to estimate the identification quality, the average μ_{err}, the standard deviation σ_{err} and the maximum max_{err} of errors between estimated and real heat fluxes are presented in Table 5 considering a Gaussian noise $\mathcal{N}(0, 0.5)$ on measured temperature.

Considering results presented in Table 5, identification performed with a constant offset equal to 15 secondes ensures an accurate identification since errors are similar to those obtained with the offline technique (Table 3.). Even if smaller time overlap reduces the delay, identification is not accurate enough.

Table 2
Temperature residuals (offline identification).

	μ_{res} (K)	σ_{res} (K)
For sensors $C_{j=(1,\ldots,10)}$	0.002	0.499

Table 3
Heat fluxes estimation errors for offline identification.

μ_{err} (W m^{-2})	σ_{err} (W m^{-2})	max_{err} (W m^{-2})
$\boldsymbol{\phi_1}$		
−37	745	3242
$\boldsymbol{\phi_2}$		
11	645	2425

This first CGM adaption (strategy S1) allows the reduction of the computation time of the identification procedure. Considering results presented in Tables 4 and 5, this method can be considering as effective. However, as shown in Fig. 7 the delay between identifications results and measurement grows up over time. In order to assess the influence of the time window choice, Table 6 is proposed.

Results presented in Table 6 show the influence of the window width on the estimation of unknown parameters quality and on the computation time. By choosing a small identification window, the unknown parameter estimations are calculated more quickly than with a larger window. Errors related to identified heat fluxes are shown in Table 7.

Results presented in Table 7 show the influence of the overlap between successive identification windows. The quality of identification results is better with a little offset (i.e. with a large overlap). Considering both Tables 6 and 7, it seems that an offset equal to the half of the window should be a correct compromise. Then in order to improve the online identification (good accuracy and small delay) and to overcome the problem of offset choice, a second strategy based on an adaptive overlap is investigated and presented in the following section.

4.3.2. Strategy 2: adaptive overlap

For this second method, the window size is constant and equal to a (for example $a = 60$ s). Let us consider the time interval $\mathcal{T}_i = [\tau_i^-, \tau_i^+] \subset T$ such as $\tau_i^+ - \tau_i^- = a$. Identification on this interval is performed during a CPU time equivalent to t_i. When the

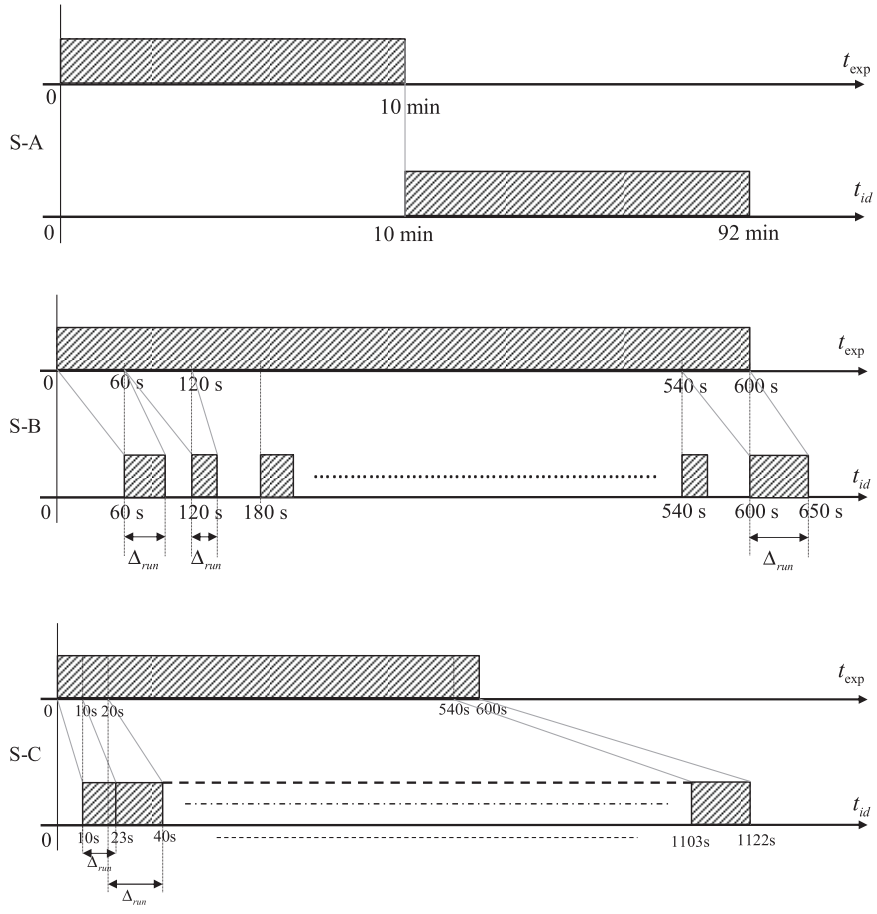

Fig. 6. Graphical representation of S–A (top); S–B (middle) and S–C strategy (bottom).

identification is satisfactory then immediately a new interval is considered $\tau_{i+1}^{+} = \tau_i^{+} + \mathrm{t}_i$ but if $\mathrm{t}_i = \tau_{i+1}^{+} - \tau_i^{+} > a$ then $\tau_{i+1}^{+} = \tau_i^{+} + b$ and $\tau_{i+1}^{-} = \tau_{i+1}^{+} - a$. Then, overlap is defined in seconds as:

$$\mathrm{Rec}(a, b, \mathrm{t}_i) = \begin{cases} a - \mathrm{t}_i & \text{if} \quad \mathrm{t}_i < a \\ a - b & \text{otherwise} \end{cases} \tag{13}$$

Table 4
Results – strategy 1.

Δt (s)	μ_{res} (K)	σ_{res} (K)	μ_{delay} (s)	t_{id} (s)	$N_{\mathscr{T}}$
15	−0.023	0.509	442	1469	37
30	−0.055	0.526	394	1426	19
45	−0.036	0.526	250	1014	13

Table 5
Heat fluxes estimation errors – strategy 1.

Δt (s)	μ_{err} (W m^{-2})	σ_{err} (W m^{-2})	max_{err} (W m^{-2})
$\boldsymbol{\phi_1}$			
15	20	547	2436
30	−161	1450	1898
45	−57	1178	3974
$\boldsymbol{\phi_2}$			
15	13	539	2369
30	−87	1005	3558
45	−53	1134	2523

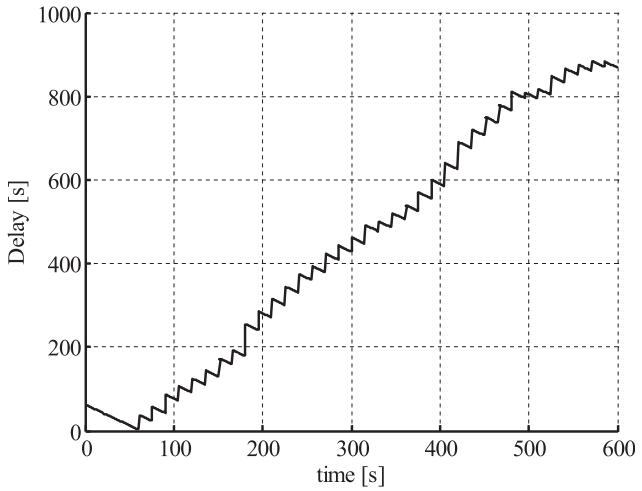

Fig. 7. Delay Δ_{run} between the identification results and measurements with ($\Delta \mathrm{t} = 15$ s) – strategy 1.

Table 6
Results for several tunings – strategy 1.

Time window size (s)	Offset Δt (s)	μ_{res} (K)	σ_{res} (K)	μ_{delay} (s)	t_{id} (s)	$N_{\mathscr{T}}$
40	10	−0.022	0.521	433	1561	57
40	20	−0.013	0.507	166	978	29
40	30	−0.027	0.530	227	1100	20
80	20	0.015	0.517	824	2341	27
80	40	0.010	0.534	447	1459	14
80	60	0.002	0.559	317	1157	10
100	25	0.005	0.516	837	2181	21
100	50	−0.005	0.561	530	1555	11
100	75	−0.037	0.598	368	1195	8

with a: the size of the identification window $\mathscr{T}_i$ and b: a fixed maximum offset.

Moreover identification process is launched only if the new measurements are not in adequacy with the temperatures predicted using the previous identification of $\phi_{1,\mathscr{T}_i}(t)$, $\phi_{2,\mathscr{T}_i}(t)$. To test the adequacy between measurements and predicted temperature on time interval $\mathscr{T}_i$, a direct problem is solved in order to compute the cost function. If measurement are in keeping with temperature calculated with the direct problem, a new time interval is considered equal to $\mathscr{T}_{i+1} = [\tau_i^{-} + t_i, \tau_i^{+} + t_i] \subset T$ with t_i is time of resolution of the direct problem.

Delays are presented in Fig. 8 for a constant window size equal to $a = 60$ s and a maximum offset equal to $b = 30$ s; such configuration is denoted by $\mathrm{Rec}(60, 30, \mathrm{t}_i)$. Temperature residuals are presented Table 8 and errors between estimated and real heat flux density are presented in Table 9.

Considering results presented in Table 8 and in Table 9, this method is relevant. The main advantage compared to the first strategy is the reduction of the total time identification procedure. Unknown parameters are identified 6 min after the end of experimentation (duration 10 min). In order to assess the influence of the time window choice, a campaign with several values of window has achieved. Results are presented in Table 10 and Table 11.

Results presented in Tables 10 and 11 show the influence of the window width and on the choice of the minimal offset on the quality of estimation of unknown parameters and on the convergence time of the identification procedure. In order to obtain a fast and accurate identification, window size has to be reduced and it seems adequate to fix a large maximum offset (in order to allow small overlap). It is obvious that too small overlap and too small window size will induce bias and there is a limit which can be define from experimental considerations. In the studied configuration, a window size equal to 60 s with a maximum offset equal to 30 s (minimum overlap is then equal to 30 s) seems to be a good compromise.

Two strategies based on initialization improvement are presented on the two following sections in order to reduce the identification time.

4.4. Initialization improvement for quasi-online identification

In this section an adaptation of previous online estimation strategies 1 and 2 is presented. This adaptation is based on an improvement in the sequential initialization of CGM. Let us consider that the next identification window is $\mathscr{T}_{i+1} = [\tau_{i+1}^{-}, \tau_{i+1}^{+}]$. Both previous methods have been implemented considering an initialization based on the last identified values on the previous time interval; see (12). In the following, initialization is based on heat fluxes derivation calculated on the previous time interval $\mathscr{T}_i$ in order to propose an initialization of the next unknown values on the next time interval $\mathscr{T}_{i+1}$. The aim of such initialization is to try to be more adequate with the previous behaviour of identified heat fluxes. Illustration is proposed on Fig. 9.

This adaption is different to the well-established Function specification Method proposed by Beck [32] which provides regularization considering a well-chosen number of future times. In our adapted CGM approach, regularization is performed considering iteration number required to reach a desired criterion (related to measurements noises). Initialization on the current investigated time window used the previous identification results but for the new instants $t \in \mathscr{T}_{i+1} = [\tau_i^{+}, \tau_{i+1}^{+}]$, unknown fluxes are identified using CGM. Below are presented results related to the adaptation of the two previous strategies (1 and 2) using this initialization improvement.

Table 7
Heat fluxes density residual for several tunings (Strategy 1).

Time window size (s)	Offset Δt (s)	ϕ_1 (W m^{-2})			ϕ_2 (W m^{-2})		
		μ_{err}	σ_{err}	max_{err}	μ_{err}	σ_{err}	max_{err}
40	10	−43	1039	3182	−8	1040	4060
40	20	−53	1771	7190	−2	1290	4989
40	30	−73	1849	5532	−51	2536	9719
80	20	−22	1119	3976	−13	808	2508
80	40	−146	1648	2509	−150	1389	3316
80	60	−155	1526	4854	−133	2006	10,892
100	25	15	883	2219	−19	821	2048
100	50	−207	1974	3629	−128	1280	3315
100	75	−210	1984	3252	−197	1977	9454

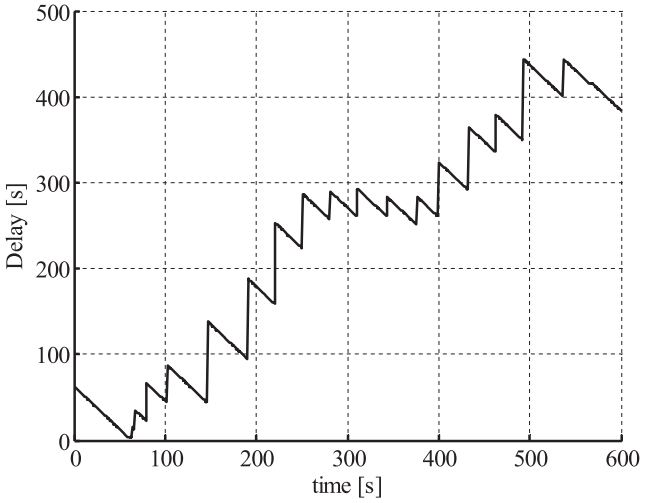

Fig. 8. Delay between measurement and identification results for "adaptive mode" – strategy 2.

Table 8
Results for strategy 2: (Rec(60, 30, t_i))

μ_{res} (K)	σ_{res} (K)	μ_{delay} (s)	t_{id} (s)	$N_{\mathcal{F}}$
−0.037	0.527	235	984	20

4.4.1. Strategy 3: constant time offset with initialization improvement

This strategy is the adaptation of the strategy 1 using initialization improvement. In order to compare this method with results of the first strategy, the same configuration (window width, offset) has been considered and results are presented in Table 12 and Table 13.

With this method, estimation results are obtained faster than with the strategy 1 and identified heat fluxes are more accurate.

4.4.2. Strategy 4: adaptive overlap and initialization improvement

This fourth strategy is the adaptation of the strategy 2 using the initialization improvement. In order to compare this method with results of the second strategy, the same configuration (window width, overlap) has been considered and results are presented in Table 14 and Table 15.

With this method estimation results are obtained faster than with strategy 2 or strategy 3 but identification results are less accurate than with strategy 3. A last identification strategy is presented below based on an adaptive choice of identification window size.

Table 10
Results for several tunings – strategy 2.

Time window size (s)	Overlap (s)	μ_{res} (K)	σ_{res} (K)	μ_{delay} (s)	t_{id} (s)	$N_{\mathcal{F}}$
40	Rec(40, 10, t_i)	−0.031	0.516	69	743	35
40	Rec(40, 20, t_i)	−0.066	0.554	139	1080	38
40	Rec(40, 30, t_i)	−0.056	0.543	94	741	35
60	Rec(60, 15, t_i)	−0.096	0.532	194	981	22
60	Rec(60, 30, t_i)	−0.037	0.527	235	984	20
60	Rec(60, 45, t_i)	−0.032	0.531	160	822	16
80	Rec(80, 20, t_i)	−0.089	0.543	355	1511	17
80	Rec(80, 40, t_i)	−0.001	0.534	417	1333	13
80	Rec(80, 60, t_i)	0.004	0.627	313	1105	10
100	Rec(100, 25, t_i)	0.000	0.526	473	1393	13
100	Rec(100, 50, t_i)	−0.029	0.546	483	1355	11
100	Rec(100, 75, t_i)	−0.037	0.598	355	1170	8

4.5. Adaptive choice of identification window size

Considering the four previous identification strategies, it has been highlighted how size and overlap of time windows are influent on the results of identification and on the delay required to obtain these results. The choice of a fixed window width can be difficult to estimate (without a priori process knowledge). In order to overcome this constraint, strategies based on an automatic selection of time interval are presented below.

4.5.1. Strategy 5: time window size related to a priori information

In order to define de time window size, the concept of *penetration time* presented in Refs. [22] and [8], can be considered. It is defined as the time that it takes for a point (here, sensor location) to be just affected by the heating boundary or source (in the current case, heating source). It is given by:

Table 9
Heat fluxes estimation errors for Strategy 2: (Rec(60, 30, t_i))

ϕ_1			ϕ_2		
μ_{err} (W m^{-2})	σ_{err} (W m^{-2})	max_{err} (W m^{-2})	μ_{err} (W m^{-2})	σ_{err} (W m^{-2})	max_{err} (W m^{-2})
−24	1170	3062	−16	976	3069

Table 11
Heat fluxes estimation errors for several tunings – strategy 2.

Time window (s)	Overlap (s)	ϕ_1 (W m^{-2})			ϕ_2 (W m^{-2})		
		μ_{err}	σ_{err}	max_{err}	μ_{err}	σ_{err}	max_{err}
40	Rec(40, 10, t$_i$)	−34	1253	2951	−20	1354	5095
40	Rec(40, 20, t$_i$)	−66	2315	10,662	−83	1845	8882
40	Rec(40, 30, t$_i$)	22	989	2767	−64	907	2469
60	Rec(60, 15, t$_i$)	−40	630	2430	−4	774	2571
60	Rec(60, 30, t$_i$)	−24	1170	3062	−16	976	3069
60	Rec(60, 45, t$_i$)	9	1022	3040	−35	1100	3738
80	Rec(80, 20, t$_i$)	−81	914	3171	−58	1127	5507
80	Rec(80, 40, t$_i$)	−103	1819	4990	−10	1134	3316
80	Rec(80, 60, t$_i$)	−283	2714	2881	−187	1501	4804
100	Rec(100, 25, t$_i$)	−6	686	1413	20	1189	3900
100	Rec(100, 50, t$_i$)	−27	1218	3629	−19	1069	3315
100	Rec(100, 75, t$_i$)	−210	1984	3252	−197	1977	9454

$$t_p = \frac{0.1}{A}\frac{d^2}{\alpha} \quad (A = 2, 3, \cdots, 10) \tag{14}$$

where $\alpha = \lambda/\rho C$ is the thermal diffusivity and d is (in the current case) the distance between the temperature sensor location and the center of the mobile source. As there are 10 sensors and two mobile sources, it is possible to compute 10 identification times (which are time dependent since distance d is varying), see Fig. 10.

In the specific situation studied in Ref. [8], with $A = 2$ the level of $10^{-A} = 1\%$ is considered and appropriate for inverse problems. Penetration times are presented in the following figure (considering measurements obtained Fig. 2 and trajectories described Fig. 1). Sensors $C_{i=1,\cdots,5}$ are dedicated to source 1 identification and sensors $C_{i=6,\cdots,10}$ are dedicated to source 2 identification. Then penetration time for $C_{i=1,\cdots,5}$ are related to S1 trajectory while penetration time for $C_{i=6,\cdots,10}$ are related to S2 trajectory.

Since both sources have to be identified during the same time window, we consider that the relevant penetration time is presented in Fig. 11 as the sum of average penetration time for each source.

Times presented Fig. 11 can be considered as an estimation of the time required for heat flux identification and is based on a priori information (material properties and heating source trajectories). However it is obvious that unknown heating flux is not taken into account in penetration time evaluation.

A $t = 0$, the penetration time presented Fig. 11 suggests that the first time window is $\mathscr{T}_1 = [0, 76]$ s. Thus measurements have to be obtained during 76 s and then the identification process is launched. At $t_{id} = 76 + 29 = 105$ identification is performed and a new time window is considered. In order to define the relevant time T, the average penetration time on [76,105] is estimated: 42 secondes. Then the new time interval is [105−42,105]. The same method is considered for new interval. However, if the new interval $\mathscr{T}_{i+1}$ does not allow an overlap, then $\mathscr{T}_{i+1} = [\tau_i^+ - 20, t_{id}]$ in order to obtain an overlap equal to 20 s.

Such strategy based on a priori information (described by penetration time) leads to the following results (see Fig. 12, Tables 16 and 17).

Previous results shows that the identification method is fast but that the accuracy is lower than previous strategies 3 or 4. Heat flux variation is not taken into account in the penetration time evaluation (14). However, sequential identification is performed and in order to adapt window size to the results obtained previously a last strategy is proposed.

4.5.2. Adaptive time window size

Let us consider the time interval $\mathscr{T}_i = [\tau_i^-, \tau_i^+] \subset T$ and dt is the time interval between measurements. A new algorithm is introduced to calculate the width of the time interval of identification. Below is presented the algorithm of the time interval for estimation procedure.

For an identification required from τ_i^-, then : $\tau_i^+ = \tau_i^-$

Do

- ***Step 1:*** *add a new measurement for the choice of window size* $\tau_i^+ = \tau_i^+ + dt$ and $\mathscr{T}_i = \left[\tau_i^-, \tau_i^+\right]$
- ***Step 2:*** *compute the cost function on interval* $\mathscr{T}_i$ *considering the predicted value of heat flux densities* $\bar{\Phi}$ *issued from* $\mathscr{T}_{i-1}$

$$J(\theta, \bar{\Phi}) = \frac{1}{2}\sum_{i=0}^{N_c}\int_{\mathscr{T}_i}\left(\theta(C_i, t; \bar{\Phi}) - \hat{\theta}_i(t)\right)^2 dt$$

- ***Step 3:*** *if* $J(\theta, \bar{\Phi}) < K.J_{Stop}$ *then goto step 1 in order to increase the measurements number*

  else launch the identification process on $\mathscr{T}_i = \left[\tau_i^-, \tau_i^+\right]$ *with* $\tau_i^+ = \max\left(\tau_i^+, \tau_i^- + 40\right)$.

Note*: Coefficient K has to be carefully chosen. First of all $K > 1$ since it is not suitable to obtain $J(\theta, \bar{\Phi}) < J_{Stop}$, see (Alifanov, et al., 1995). For large value of K, identification is rarely performed and method looks like offline approach. For $K \approx 1$, identification is too often required and CPU time for identification induces a large delay. In the following results are shown for $K = 3$.*

The window's size is modified online according to the previous algorithm and additional direct problem resolution is required in order to estimate if new measurements are in adequacy with predicted heating flux densities. Two strategies are developed and

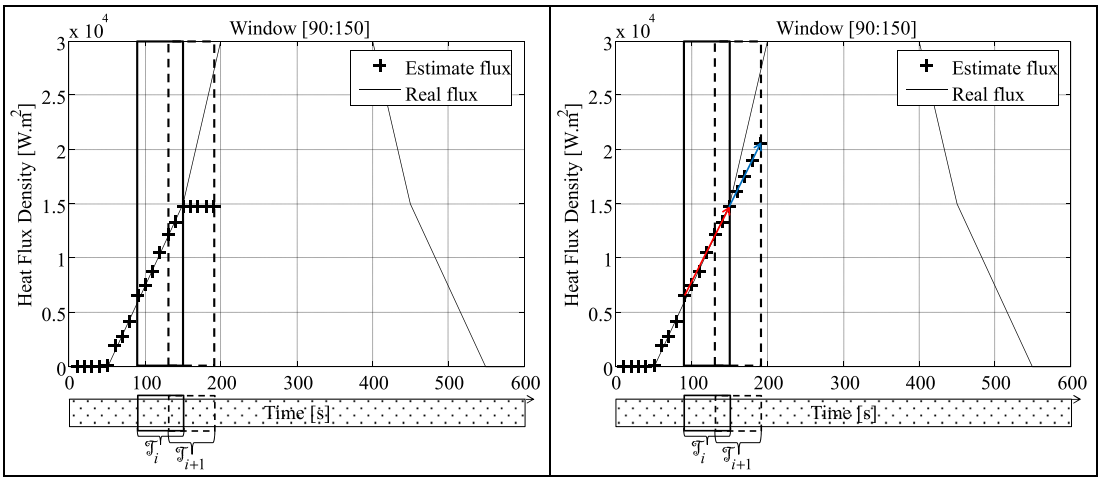

Fig. 9. Example of initialization improvement on the next time interval $\mathcal{T}_{i+1}$.

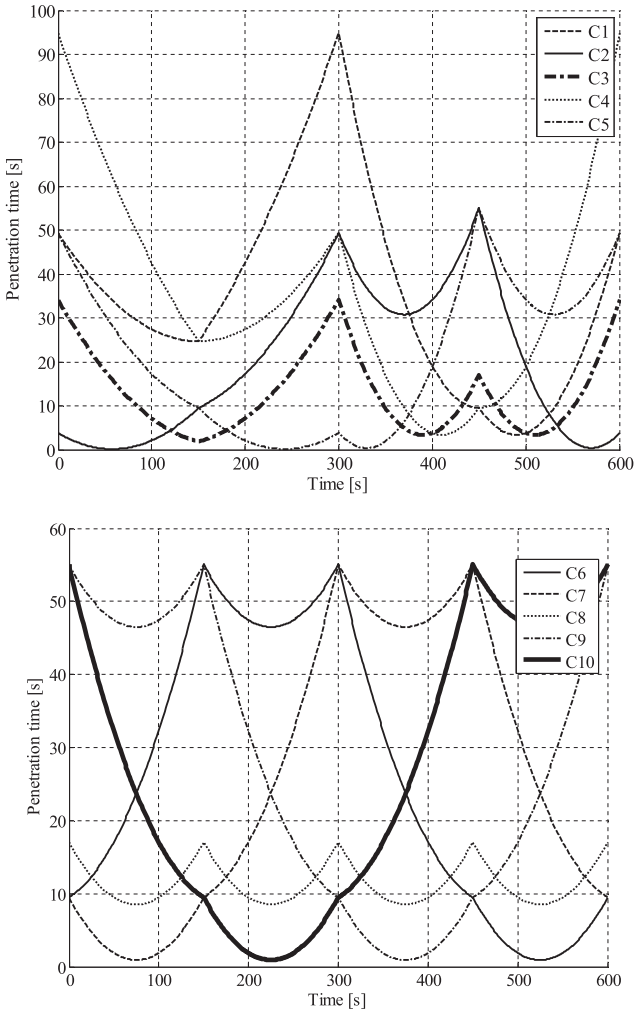

Fig. 10. Penetration times for sensors $C_{i=1,\cdots,5}$ and sensors $C_{i=6,\cdots,10}$.

Table 12
Results for several tunings – strategy 3.

Time window size (s)	Offset Δt (s)	μ_{res} (K)	σ_{res} (K)	μ_{delay} (s)	t_{id} (s)	$N_{\mathcal{T}}$
40	10	−0.004	0.509	121	793	57
40	20	−0.008	0.516	92	739	29
40	30	−0.008	0.516	38	603	20
60	15	−0.017	0.514	108	727	37
60	30	−0.050	0.506	70	638	19
60	45	−0.012	0.512	78	645	13
80	20	−0.013	0.505	194	896	27
80	40	0.003	0.506	120	692	14
80	60	0.011	0.513	150	737	10
100	25	−0.002	0.518	378	1210	21
100	50	−0.024	0.520	315	1039	11
100	75	−0.012	0.527	249	1025	8

Table 13
Heat fluxes estimation errors for several tunings – strategy 3.

Time window size (s)	Offset Δt (s)	ϕ_1 (W m^{-2})			ϕ_2 (W m^{-2})		
		μ_{err}	σ_{err}	max_{err}	μ_{err}	σ_{err}	max_{err}
40	10	8	616	1999	−32	821	4142
40	20	−13	995	2943	−14	1150	6464
40	30	−43	1514	4724	26	907	2812
60	15	−30	329	992	44	864	3873
60	30	−20	790	2457	−15	427	1694
60	45	−2	1291	3060	−20	562	2166
80	20	−29	329	992	44	864	3873
80	40	−20	790	2457	−15	427	1694
80	60	−2	1291	3060	−20	562	2166
100	25	6	14	681	386	2342	1067
100	50	−36	10	765	549	2742	2090
100	75	−3	4	999	425	3385	1540

presented below. These identification procedures are based on strategies 3 and 4 presented in (4.3.1) and (4.3.2).

4.5.3. Strategy 6: identification with adaptive time window size and constant offset

This strategy is based on principle proposed in strategy 3 with the adaptive selection of time window size presented in 4.5.2.

Table 14
Results for several tunings – strategy 4.

Time window size (s)	Overlap (s)	μ_{res} (K)	σ_{res} (K)	μ_{delay} (s)	t_{id} (s)	$N_{\mathcal{F}}$
40	Rec(40, 10, t_i)	0.018	0.519	58	685	61
40	Rec(40, 20, t_i)	−0.027	0.529	47	666	72
40	Rec(40, 30, t_i)	0.046	0.545	37	630	67
60	Rec(60, 15, t_i)	−0.059	0.542	127	859	36
60	Rec(60, 30, t_i)	−0.027	0.526	118	803	26
60	Rec(60, 45, t_i)	−0.028	0.538	86	716	28
80	Rec(80, 20, t_i)	0.010	0.514	216	927	18
80	Rec(80, 40, t_i)	−0.025	0.522	126	736	24
80	Rec(80, 60, t_i)	0.040	0.518	148	794	13
100	Rec(100, 25, t_i)	−0.020	0.539	321	1054	11
100	Rec(100, 50, t_i)	−0.081	0.535	259	893	9
100	Rec(100, 75, t_i)	−0.001	0.566	267	893	8

Constant time offset is half of the considered time interval. Results are presented below in (Fig. 13) and Tables 18 and 19.

In regarding to the results of temperature residuals and identification results of unknown parameters, this method brings an interesting advantage on the difficulty of choice of time interval width. Final identification time is reduced but average delay is greater than the previous method.

4.5.4. Strategy 7: identification with adaptive time window size and adaptive overlap

This strategy is based on principle proposed in strategy 4 with the adaptive selection of the time window size presented in 4.5.2. Results are presented below in (Fig. 14) and Tables 20 and 21.

This last method leads to a reliable identification of heat fluxes (see Tables 20 and 21 and Fig. 15) with final results obtained 23 s after the experimentation. Considering results of temperature residuals and on the estimation quality of unknown parameters, this last strategy can be considerate as the most successful achievement since identification is accurate and that average delay between a measure and an identification result is about 1 min.

5. Concluding remarks

In this paper, several approaches for identification of heat fluxes provided by two mobile sources on a thin metallic plate have been presented. These strategies are based on the Conjugate Gradient Method (CGM) known for its effectiveness on ill-posed inverse problems described by partial differential equations such as inverse heat conduction problem. Ten fixed sensors

Table 15
Heat fluxes estimation errors for several tunings – strategy 4.

Time window size (s)	Overlap (s)	ϕ_1 (W m^{-2})			ϕ_2 (W m^{-2})		
		μ_{err}	σ_{err}	max_{err}	μ_{err}	σ_{err}	max_{err}
40	Rec(40, 10, t_i)	−18	653	1562	35	770	4287
40	Rec(40, 20, t_i)	−36	542	1219	16	903	4287
40	Rec(40, 30, t_i)	70	671	3427	7	937	4287
60	Rec(60, 15, t_i)	25	2011	12,906	−56	1718	8892
60	Rec(60, 30, t_i)	0	2029	12,629	23	553	1734
60	Rec(60, 45, t_i)	80	2066	10,403	−60	827	1933
80	Rec(80, 20, t_i)	−3	659	1975	25	428	1427
80	Rec(80, 40, t_i)	6	567	1799	1	391	952
80	Rec(80, 60, t_i)	3	838	2549	16	299	762
100	Rec(100, 25, t_i)	−29	774	2754	38	605	2021
100	Rec(100, 50, t_i)	−55	830	2329	−40	524	947
100	Rec(100, 75, t_i)	−36	716	1874	58	1162	4330

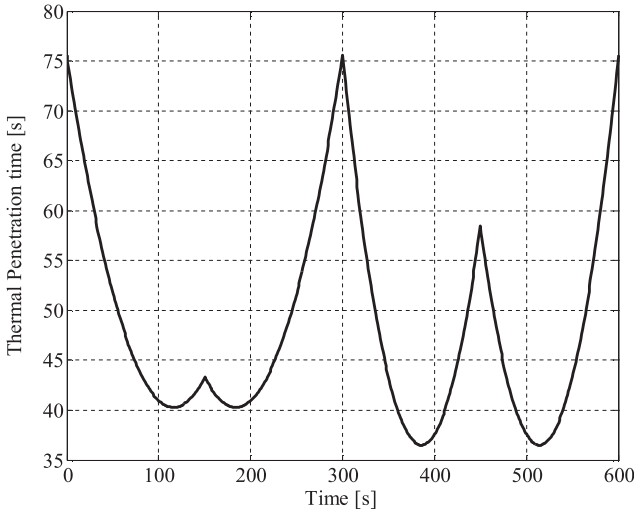

Fig. 11. Global penetration times.

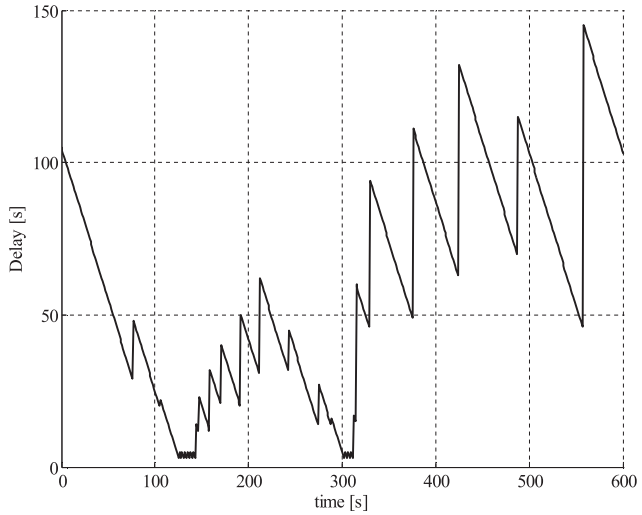

Fig. 12. Delay between the identification results and measurement with Penetration time strategy.

Table 16
Results – strategy 5.

μ_{res} (K)	σ_{res} (K)	μ_{delay} (s)	t_{id} (s)	$N_{\mathcal{F}}$
−0.081	0.59	62	703	28

Table 17
Heat fluxes estimation errors – strategy 5.

ϕ_1			ϕ_2		
μ_{err} (W m^{-2})	σ_{err} (W m^{-2})	max_{err} (W m^{-2})	μ_{err} (W m^{-2})	σ_{err} (W m^{-2})	max_{err} (W m^{-2})
31	392	999	−44	428	1318

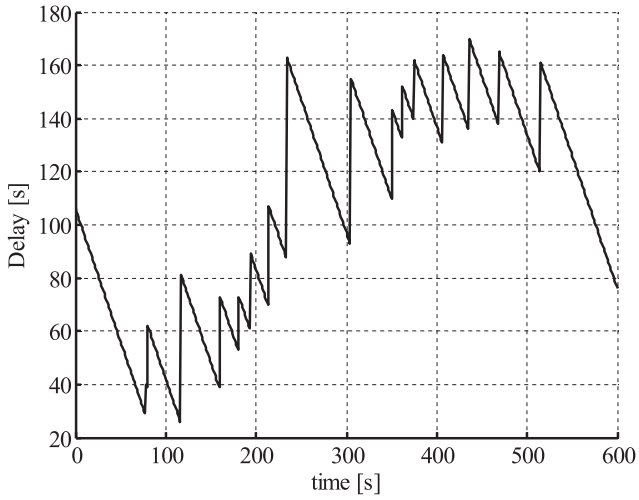

Fig. 13. Delay between the identification results and measurement with strategy 5.

Table 18
Results – strategy 6.

μ_{res} (K)	σ_{res} (K)	μ_{delay} (s)	t_{id} (s)	$N_{\mathcal{F}}$
−0.052	0.53	108	676	17

located in the mobile sources neighbourhood provide pointwise temperature measurement each second for heat fluxes identification (118 unknown parameters). Experimentation duration is 10 min. Several strategies are proposed and their effectiveness is shown considering both the time required for identification and the results quality. In the studied case, offline CGM provides relevant results 82 min after the end of the process. In order to ensure a faster (but accurate) identification, several strategies are based on the choice of the measurements taken into account for

Table 19
Heat fluxes estimation errors – strategy 6.

ϕ_1			ϕ_2		
μ_{err} (W m^{-2})	σ_{err} (W m^{-2})	max_{err} (W m^{-2})	μ_{err} (W m^{-2})	σ_{err} (W m^{-2})	max_{err} (W m^{-2})
−33	563	1874	9	620	2268

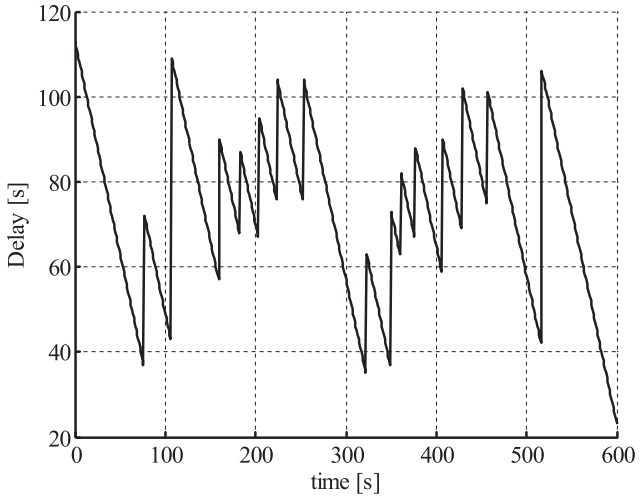

Fig. 14. Delay between the identification results and measurement with strategy 7.

Table 20
Results – strategy 7.

μ_{res} (K)	σ_{res} (K)	μ_{delay} (s)	t_{id} (s)	$N_{\mathcal{F}}$
−0.017	0.51	73	623	17

Table 21
Heat fluxes estimation errors – strategy 7.

ϕ_1			ϕ_2		
μ_{err} (W m^{-2})	σ_{err} (W m^{-2})	max_{err} (W m^{-2})	μ_{err} (W m^{-2})	σ_{err} (W m^{-2})	max_{err} (W m^{-2})
−19	603	1649	16	427	1281

identification (i.e. the limits of the time integral for direct, adjoint and sensitivity problem). A shorter interval provides quick convergence (before the experimentation end) and an overlap with the next interval allows an accurate identification. Several strategies are tested in order to deal with overlap and sliding (receding) time window size. An a priori consideration related to

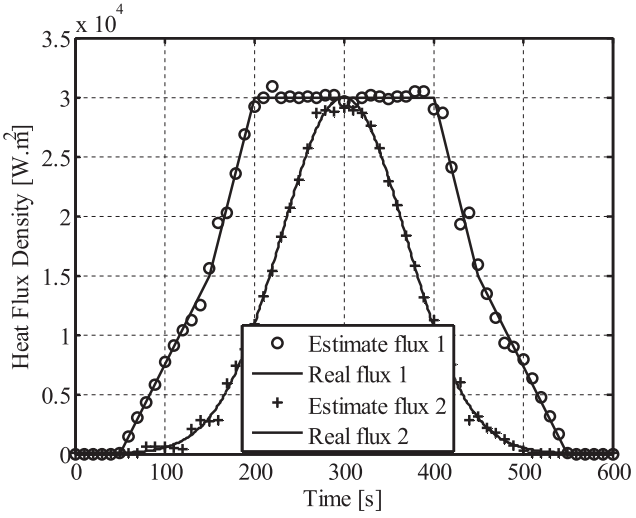

Fig. 15. Identified heat fluxes with strategy 7.

thermal penetration time is also tested. The best strategy offers a quasi-online identification which ensures a reliable identification only 23 s after the end of the process. Moreover the average delay between online observation and parameter identification is 73 s. The main limitation of this approach is the processor performance and then this delay will be sharply reduced in the next few years.

Thus, adaptive control law based on closed loop can be investigated since heat fluxes variation can be detected using such quasi online identification approach (for continuous production process for example). Such delay systems are widely studied in control theory.

Acknowledgement

This work was partially supported by the ANR-12-BS03-008-03.

References

[1] O.M. Alifanov, Solution of an inverse problem of heat-conduction by iterative methods, J. Eng. Phys. 26 (4) (1974) 471–476.
[2] O.M. Alifanov, E.A. Artiukhin, S.V. Rumiantsev, Extreme Methods for Solving Ill-posed Problems with Applications to Inverse Heat Transfer Problems, Begell House, New-York, 1995.
[3] R.C. Aster, B. Borchers, C.H. Thurber, Parameter Estimation and Inverse Problems, second ed., Academic Press, Waltham, 2013.
[4] J.V. Beck, K.J. Arnold, Parameter Estimation in Engineering and Science, John Wiley & Sons Edition, 1977.
[5] S. Beddiaf, L. Autrique, L. Perez, J.C. Jolly, Time-dependent heat flux identification: application to a three-dimensional inverse heat conduction problem, in: Wuhan- China, 4th Int. Conf. on Modelling, Identification and Control, 2012.
[6] S. Beddiaf, L. Perez, L. Autrique, J.-C. Jolly, Simultaneous determination of time-varying surface heat flux and location of a fixed source in a three-dimensional domain, Int. J. Inverse Probl. Sci. Eng. (2013).
[7] Y.Q. Chen, C. Tricaud, Optimal interlaced mobile sensor motion planning and parameter estimation for distributed parameter systems, in: Proceedings of 2008 Engineering Research and Innovation Conference, Knoxville, Tennessee, USA, 2008.
[8] K.D. Cole, J.V. Beck, K.A. Woodbury, Filippo de Monte, Intrinsic verification and a heat conduction database, Int. J. Therm. Sci. 78 (2014) 36–47.
[9] N. Daouas, M.-S. Radhouani, A new approach of the Kalman filter using future temperature measurements for nonlinear inverse heat conduction problem, Numer. Heat. Transf. Part B. 45 (2004) 565–585.
[10] N. Daouas, M.-S. Radhouani, Experimental validation of an extended Kalman smoothing technique for solving nonlinear inverse heat conduction problems, Inverse Probl. Sci. Eng. 15 (7) (2007) 765–782.
[11] K.-J. Dowding, J.V. Beck, A sequential gradient method for the inverse heat conduction problem (IHCP), J. Heat Transf. 121 (1999) 300–306.
[12] H. Egger, Y. Heng, W. Marquardt, A. Mhamdi, Efficient solution of a three-dimensional inverse heat conduction problem in pool boiling, Inverse Probl. 25 (2009), 095006 (19pp).
[13] E. Fridman, Introduction to Time-delay Systems: Analysis and Control. Series: Systems & Control: Foundations & Applications, s.l.:Birkhäuser Basel, 2014.
[14] J. Gaspar, et al., Nonlinear heat flux estimation in the JET divertor with the ITER like wall, Int. J. Therm. Sci. 72 (2013) 82–91.
[15] A. Hasanov, B. Pektas, Identification of an unknown time-dependent heat source term from overspecified Dirichlet boundary data by conjugate gradient method, Comput. Math. Appl. 65 (1) (2013) 42–57.
[16] C. Huang, W. Chen, A 3D inverse forced convection problem in estimating surface heat flux by conjugate gradient method, Int. J. Heat Mass Transf. 43 (2000) 317–3181.
[17] V. Isakov, Inverse Problems for Partial Differential Equtions, Springer-Verlag, New-York, 1998.
[18] Y. Jarny, M.N. Ozisik, J.P. Bardon, A general optimization method using adjoint equation for solving multidimensional inverse heat conduction, Int. J. Heat Mass Transf. 34 (11) (1991) 2911–2919.
[19] L. Ling, Y. Yamamoto, Y. Hon, T. Takeuchi, Identification of source locations in two-dimensional heat equations, Inverse Probl. 22 (2006) 1289–1305.
[20] L.A. Martinez-Gomez, A. Weitzenfeld, Real time vision system for a small size league team, in: Mexico, Proceedings of the 1st IEEE Latin American Robotics Symposium, 2004.
[21] M. Mohammadiun, A.B. Rahimi, I. Khazaee, Estimation of the time-dependent heat flux using the temperature distribution at a point by conjugate gradient method, Int. J. Therm. Sci. 50 (12) (2011) 2443–2450.
[22] F. de Monte, J.V. Beck, D.E. Amos, Diffusion of thermal disturbances in two-dimensional Cartesian transient heat conduction, Int. J. Heat Mass Transf. 51 (25–26) (2008) 5931–5941.
[23] F. de Monte, J.V. Beck, D.E. Amos, A heat-flux based building block approach for solving heat conduction problems, Int. J. Heat Mass Transf. 54 (13–14) (2011) 2789–2800.
[24] L. Perez, Observation strategies for mobile heating source tracking. Albi, in: 4th Inverse Problems, Design and Optimization Symposium, 2013, ISBN 979-10-91526-01-2.
[25] L. Perez, L. Autrique, M. Gillet, Implementation of a conjugate gradient algorithm for thermal diffusivity identification in a moving boundaries system, J. Phys. 135 (2008).
[26] H.-J. Reinhardt, Analysis of sequential methods solving the inverse heat conduction problem, Numer. Heat. Transf. Part B. 4 (1993) 455–474.
[27] H.-J. Reinhardt, Dinh Nho Hào, A sequential conjugate gradient method for the stable numerical solution to inverse heat conduction problems, Inverse Probl. Eng. 2 (4) (1996) 263–272.
[28] S. Rouquette, L. Autrique, C. Chaussavoine, L. Thomas, Identification of influence factors in a thermal model of a plasma-assisted chemical vapor deposition process, Inverse Probl. Sci. Eng. 15 (5) (2007) 489–515.
[29] A. Tarantola, Inverse Problem Theory and Methods for Model Parameter Estimation, Society for Industrial and Applied Mathematics, Philadelphia, 2005.
[30] A. Vergnaud, P. Lucidarme, L. Autrique, L. Perez, Adaptive deployment of a mobile sensors network to optimize the monitoring of a phenomenon governed by partial differential equations. Reykjavik, in: 10th International Conference on Informatics in Control, Automation and Robotics, 2013.
[31] E. Videcoq, D. Petit, Model reduction for the resolution of multidimensional inverse heat conduction problems, Int. J. Heat Mass Transf. 44 (10) (2001) 1899–1911. May 2001.
[32] K.A. Woodbury, Inverse Engineering Handbook, CRC Press, 2002, p. 480.
[33] J. Zhou, Y. Zhang, J.K. Chen, Z.C. Feng, Inverse estimation of surface heating condition in a three-dimensional object using conjugate gradient method, Int. J. Heat Mass Transf. 53 (13–14) (2010) 2643–2654.
[34] S. Zickler, et al., SSL-vision: the shared vision system for the RoboCup small size league, in: GR, SJ, WW (Eds.), RoboCup 2009 Robot Soccer World Cup XIII. s.l.:Springer, 2009, pp. 437–474.